

## ORIENTED GROWTH OF APATITE-LIKE CRYSTALS AT THE INTERFACE BETWEEN A SILICATE NANOCOMPOSITE AND SIMULATED BODY FLUID

F. TALOS<sup>1,2</sup>, A. VULPOI<sup>1</sup>, A. PONTON<sup>2</sup>, S. SIMON<sup>1\*</sup>, D. DUDEA<sup>3</sup>, S. BRAN<sup>3</sup>

<sup>1</sup> Babes-Bolyai University, Faculty of Physics & Institute for Interdisciplinary Research in Bio-Nano-Sciences, 400084 Cluj-Napoca, Romania

<sup>2</sup> Laboratory MSC, UMR 7057, Univ Paris Diderot, CNRS, Bât. Condorcet, CC 7056, 75205 Paris Cedex 13, France

<sup>3</sup> University of Medicine and Pharmacy "Iuliu Hațieganu", Faculty of Dental Medicine, 400029 Cluj-Napoca, Romania

Calcium pyrophosphate nanocrystals incorporated in an amorphous silica based matrix were obtained by sol-gel process followed by heat treatment applied at 550 °C. The resulted nanocomposite was characterized by X-ray diffraction (XRD), Fourier Transform Infrared Spectroscopy (FTIR), Scanning Electron Microscopy (SEM) and Energy Dispersive Spectroscopy (EDS). The surface reactivity of the nanocomposite was investigated in simulated body fluid (SBF) at 37°C up to 21 days. The results point out that the calcium pyrophosphate nanocrystals induce the oriented growth of bioactive apatite-like crystals on the surface of the investigated nanocomposite.

(Received December 18, 2012; Accepted January 20, 2013)

*Keywords:* nanocomposites, calcium pyrophosphate, SBF, apatite-like phase.

### 1. Introduction

In the last decade glass-ceramics, composites and polymers have been used to repair or reconstruct parts of the injured osseous tissue and several studies were reported about the interaction of these materials with the surrounding tissue [1-5]. The apatite-like layer developed on the surface of bioactive materials in simulated body fluid can promote chemical bond in contact with living tissue [3]. The bioactive behaviour of materials depends on their chemical composition, structure and surface chemistry. There are requirements imposed to materials considered for medical applications in bone repair highly target their bioactivity [6-9]. In order to achieve such bioactivity for glass-ceramics, largely used in scaffolds for tissue regeneration, [10], the sol-gel method became preferred to the classical melt-quenching method of glasses [11-14] because of the high purity and homogeneity control and the relatively low synthesis temperature.

This paper is focused on synthesis, structural and morphological characterization of a new SiO<sub>2</sub>-CaO-P<sub>2</sub>O<sub>5</sub> nanocomposite, and on its bioactivity proven *in vitro*.

### 2. Materials and methods

#### 2.1 Sample preparation

The sol-gel derived 60.6SiO<sub>2</sub>-30.3CaO-9.1P<sub>2</sub>O<sub>5</sub> (mol %) sample was prepared using reagents in ratios given in Table 1.

---

\*Corresponding author: simons@phys.ubbcluj.ro

Table 1. The ratio of the reagents used in hydrolysis-condensation reactions.

HNO <sub>3</sub> concentr. (M)	TEOS/EtOH	H <sub>2</sub> O/HNO <sub>3</sub> /EtOH	Ca(NO <sub>3</sub> ) <sub>2</sub> •4H <sub>2</sub> O /H <sub>2</sub> O/HNO <sub>3</sub>	(NH <sub>4</sub> ) <sub>2</sub> HPO <sub>4</sub> /H <sub>2</sub> O/HNO <sub>3</sub>
1	1.02/2.04	0.22/0.17/0.31	0.51/1.02/0.085	0.43/0.86/0.085

Tetraethyl orthosilicate TEOS, (Si (OC<sub>2</sub>H<sub>5</sub>)<sub>4</sub>, Merck), calcium nitrate (Ca (NO<sub>3</sub>)<sub>2</sub>•4H<sub>2</sub>O, VWR Prolabo) and di-ammonium hydrogen phosphate ((NH<sub>4</sub>)<sub>2</sub>HPO<sub>4</sub>, VWR Prolabo), were the reagents used in the synthesis process. The selected catalyst was the nitric acid (HNO<sub>3</sub>, Merck). The solvent chosen for TEOS was its parent alcohol, the ethanol (C<sub>2</sub>H<sub>6</sub>O, EtOH) and the polymerizing reactant was deionized water. All the reagents and solvents were analytical-grade quality, purchased commercially and used without any further purification. Tetraethyl orthosilicate (TEOS, (Si (OC<sub>2</sub>H<sub>5</sub>)<sub>4</sub>) was mixed with EtOH on a magnetic stirrer at 400 rpm during 30 minutes. To trigger the reactions of TEOS another liquid media, H<sub>2</sub>O, was added. All the hydrolysis reactions of the reagents were performed at room temperature. The calcium and phosphorus salts were separately dissolved in deionised water and stirred for 30 minutes. The further addition of phosphorus into calcium solution induced a white precipitate. Nitric acid was added to this white precipitate. Afterwards the TEOS/EtOH/H<sub>2</sub>O/HNO<sub>3</sub> solution was added drop wise into Ca (NO<sub>3</sub>)<sub>2</sub>•4H<sub>2</sub>O/ (NH<sub>4</sub>)<sub>2</sub>HPO<sub>4</sub>/ HNO<sub>3</sub> mixture under continuous stirring for 1 hour at 37 °C keeping the pH constant at 1. The obtained gel was dried and thermal treated at 550 °C for 1 hour.

## 2. 2 Experimental techniques

The structural changes induced by heat treatment and SBF soaking were investigated by X-ray diffraction using a Shimadzu XRD-6000 diffractometer with a monochromator of graphite for CuK $\alpha$  ( $\lambda=1.54$  Å). The diffractograms were recorded in 2 $\theta$  range from 10° to 70° with a speed of 2°/min.

The FTIR spectra were recorded at room temperature in the 400 - 4000 cm<sup>-1</sup> spectral range in absorbance mode with a JASCO FT/IR-6200 spectrometer, with an instrumental resolution of 4 cm<sup>-1</sup> and averaging of 256 scans. An amount of 0.8 mg of powder sample was thoroughly mixed with 150 mg of KBr and compressed under 100 N/mm<sup>2</sup> to form pellets.

FEI QUANTA 3D FEG dual beam scanning electron microscope with Everhart-Thornley detector was used to analyze the microstructure and morphology of the vitrocereamics before and after SBF immersion. In order to amplify the secondary electrons signal a cover of 5 nm thickness was performed with Pt-Pd into Agar Automatic Sputter Coater, in Ar atmosphere.

The bioactivity of the glass powder was evaluated under static conditions in simulated body fluid (SBF), the Kokubo's balanced salt solution with ionic concentration nearly equal to the human blood plasma [15]. Batches of 150 mg glass-ceramic powder were put in polyethylene recipients with 15 mL of SBF and kept in incubator at 37°C. The recipients were then removed from the incubator at different time periods: 1, 6, 24 hours and 21 days respectively. The samples were removed from the fluid, rinsed with ultrapure water, dried at room temperature and investigated by X-ray diffraction, FTIR spectroscopy and SEM.

## 3. Results and discussion

The XRD patterns of the vitrocereamic sample before and after SBF immersion up to 21 days (Fig. 1) show a calcium pyrophosphate Ca<sub>2</sub>P<sub>2</sub>O<sub>7</sub> (PDF card 73-0440, JCPDS) nanocrystalline phase after the 550 °C heat treatment. The crystallites size determined according to Scherrer formula [16] is around 13 nm. The X-ray diffractograms recorded from samples soaked in SBF reveal the presence of the new peaks at 2 $\theta$  close to 26° and 32°. These new peaks correspond to

(002) and (211) reflections of hydroxyapatite phase (PDF card 09-0432, JCPDS). In order to clearly distinguish the hydroxyapatite phase, the standard pattern of HA was inserted in Fig. 1.

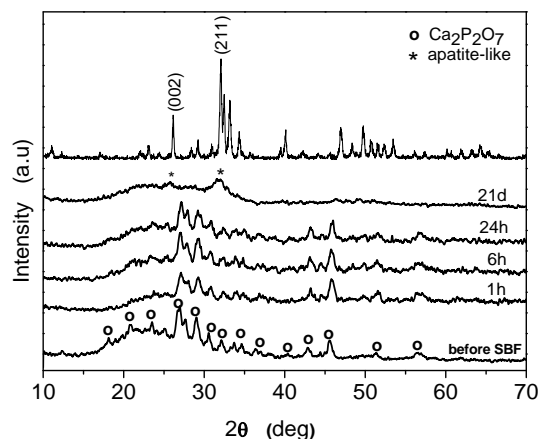


Fig. 1. XRD patterns of 550 °C heat treated sample before and after soaking in SBF.

The depolymerisation of the silicate network due to SBF immersion was investigated by FTIR analysis. The FT-IR spectra (Fig. 2) are dominated by strong absorption bands, associated to vibrational modes of SiO<sub>4</sub> and PO<sub>4</sub> tetrahedras, which are overlapped.

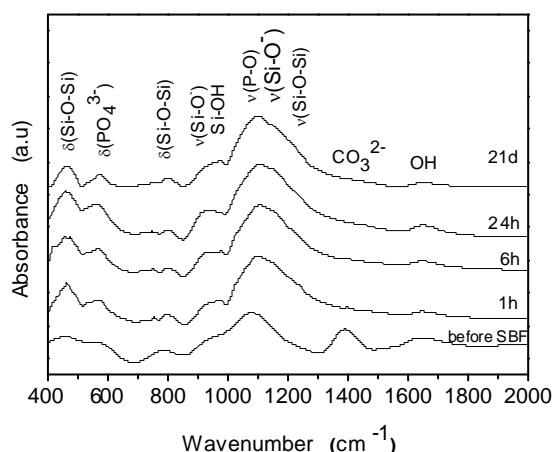
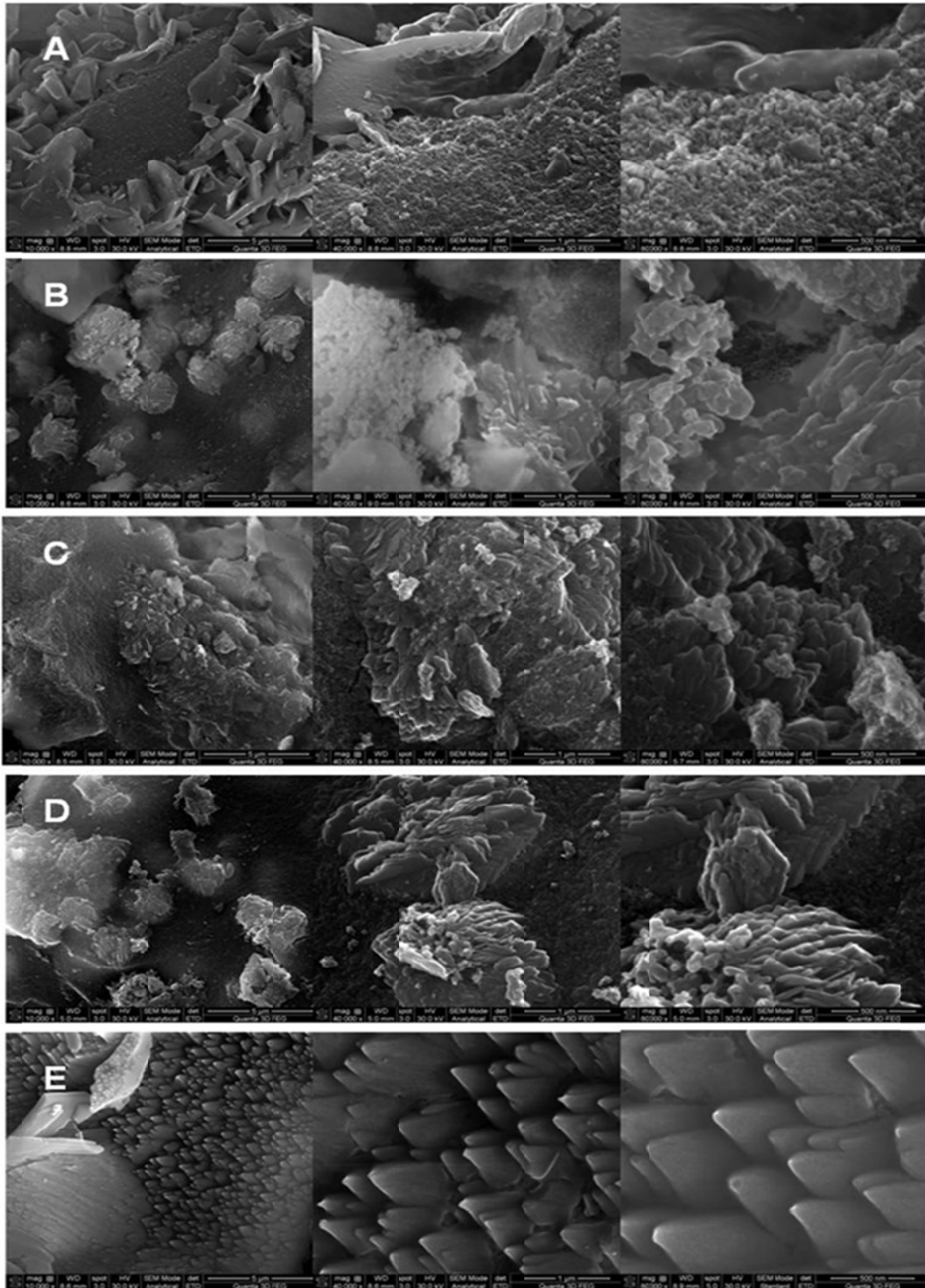


Fig. 2. FTIR spectra of the sample annealed at 550 °C before and after incubation in SBF.

The shoulder at 1205 cm<sup>-1</sup> is ascribed to the longitudinal optical Si-O-Si stretching mode and the band near 1100 cm<sup>-1</sup> is attributed to the stretching vibration of Si-O<sup>-</sup> bonds [17]. The absorption bands near 1040 cm<sup>-1</sup> and 575 cm<sup>-1</sup> are assigned to the vibration mode of the tetrahedral PO<sub>4</sub><sup>3-</sup> present in hydroxyapatite [18] gradually increases by increasing the immersion period. Further, the vibration at 960 cm<sup>-1</sup> ascribed to Si-OH groups [19] was overlapped on the bands corresponding to Si-O<sup>-</sup> groups, became larger after 21 days of SBF immersion pointing out the gradual depolymerisation of silica matrix [20]. A weak band which arise at about 800 cm<sup>-1</sup> can be associated to the bending motion of oxygen atoms along the bisector of the Si-O-Si bridging group [21]. Another strong band was also observed at 466 cm<sup>-1</sup> ascribed to rocking motion of the bridging oxygen atoms perpendicularly to the Si-O-Si plane [22]. FTIR analysis of studied samples showed the slight decrease in absorbance of Si-O while the vibration bands due to phosphates steadily increased. In addition, stretching vibration mode due to carbonates and hydroxyl groups [19] were observed close to 1400 and 1600 cm<sup>-1</sup>, respectively. The band due to carbonates groups disappears once with the increase of immersion period.

The presence of apatite-like nanocrystalline phase confirmed by XRD analysis is in good agreement with the SEM images (Fig.3). From these images one can observe the gradual surface

changes by increasing the immersion time. The thermal treated sample presents large calcium pyrophosphate crystals (Fig. 3(A)).



*Fig. 3. SEM images recorded before (A) and after different periods of SBF incubation: (B) 1 hour, (C) 6 hour, (D) 24 hour, (E) 21 days.*

It should be noticed that after 1 hour of SBF incubation first of all the calcium amount on the sample surface increases (Fig. 4).

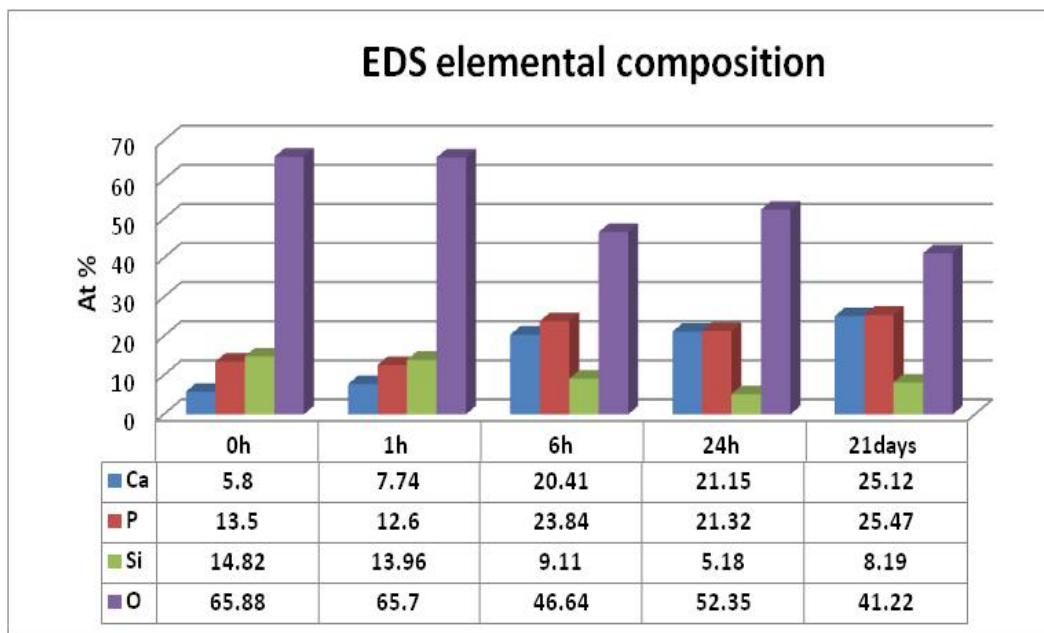


Fig. 4. EDS elemental concentrations of the silicate-calcium-phosphate nanocomposite before and after immersion in SBF from 1 hour to 21 days.

Considering that the functional groups for apatite nucleation are negatively charged in physiological solutions, calcium incorporation in the initial stage is very important for apatite nucleation [23-24].

The dependence of the elemental composition, estimated by EDS, function on SBF immersion time is given in Fig. 5.

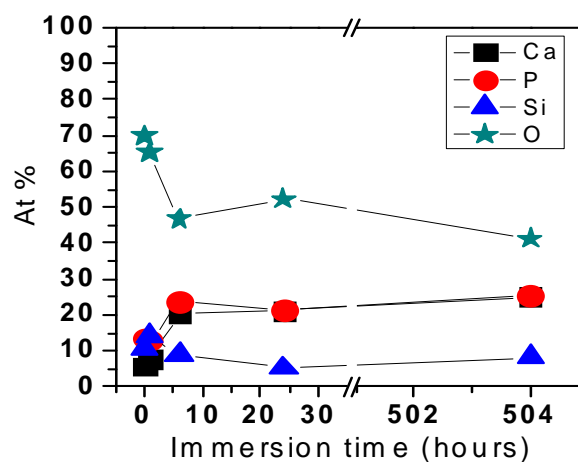


Fig. 5. The elemental concentrations determined by EDS after different SBF immersion time.

One can observe that the silicon content in the first hour of incubation decreases and afterwards up to 21 days (506 hours) presents a slight increase. The calcium and phosphorus concentrations have an opposite evolution to the silicon, with changes more pronounced from 1 hour to 6 hours.

The Ca/P ratio increases with the immersion time inducing the development of spherical islands of crystallites on the sample surface (Fig. 3). The presence of silanol (Si-OH) groups on material surface as well the increase of Ca/P ratio up to 21 days of immersion produce heterogeneous nucleation of apatite-like crystals. These results indicate that not only the numbers of functional groups revealed by FTIR analysis but also their arrangement are important factors that govern apatite formation. Further, the SEM images after 21 days of SBF immersion display a preferential orientation of the crystals growing (Fig. 3(E)). The apatite-like crystals, around 200-500 nm in size, present a spectacular, needle morphology.

#### 4. Conclusions

The composite obtained by 550 °C heat treatment of 60.6SiO<sub>2</sub>·30.3CaO·9.1P<sub>2</sub>O<sub>5</sub> sol-gel derived bioactive glass consists of a nanocrystalline calcium pyrophosphate phase developed in the amorphous silica rich matrix. The incubation of the composite in simulated body fluid lead to gradual appearance of the phosphate groups as proved by both FTIR and EDS analysis. A spectacular result is the growth of preferentially orientated apatite-like crystals at the interface of the studied nanocomposite with the simulated body fluid. The presence of calcium pyrophosphate nanocrystalline phase appears as an excellent support for development of bioactive apatite-like nanocrystals that could enhance oriented growth of regenerated mineral bone phase.

#### Acknowledgments

This research was accomplished in the framework PNII IDEI - PCCE 101/2008 PROJECT granted by the Romanian National University Research Council -CNCSIS. F. Taloş author wishes to thank for the financial support provided from programs co-financed by the Sectoral Operational Programme Human Resources Development POSDRU/88/1.5/S/60185-INNOVATIVE DOCTORAL STUDIES IN A KNOWLEDGE BASED SOCIETY. The authors D. Dudea and S. Bran contributed equally to this work.

#### References

- [1] L.L Hench, *Biomaterials* **19**, 1419 (1998).
- [2] L.L Hench, J. Wilson, *Science*, **226**, 630 (1984).
- [3] L.L Hench, *J. Mater. Sci. Med.* **17**, 967 (2006).
- [4] S.V. Dorozhkin, *Acta Biomater.* **8**, 963 (2012).
- [5] S. Simon, R.V.F. Turcu, T. Radu, M. Moldovan, V. Simon, *J. Optoelectron. Adv. Mater.* **11**, 1660 (2009).
- [6] S.I. Roohani-Esfahani, S. Nouri-Khorasani, Z.F. Lu, R.C. Appleyard, H. Zreiqat, *Acta Biomater.* **7**, 1307 (2011).
- [7] A.J. Nathanael, J.H. Lee, D. Mangalaraj, S.I. Hong, Y.H. Rhee, *Powder Technol.* **228**, 410 (2012).
- [8] K.C.R. Kolan, M.C. Leu, G.E. Hilmas, M. Velez, *J. Mech. Behav. of Biomed. Mater.* **13**, 14 (2012).
- [9] A. Vulpoi, L. Baia, S. Simon, V. Simon, *Mater. Sci. Eng. C* **32**, 178 (2012).
- [10] M.A. Matsumoto, G. Caviquioli, C.C. Bigueti, L. de Andrade Holgado, P. Pinto Saraiva, A.Cl. Muniz Renno, R. Yoshio Kawakami, *J. Mater. Sci. Mater. Med.* **23**, 1447 (2012).
- [11] S. Simon, R. Ciceo-Lucacel, T. Radu, L. Baia, O. Ponta, A. Iepure, V. Simon, *J. Mater. Sci. Mater. Med.* **23**, 1193 (2012).
- [12] V. Simon, M. Todea, S. Simon, *Int. J. Mod. Phys. B*, **19**, 3293 (2005).

- [13] G. Voicu, A.I. Badanoiu, C.D. Ghitulica, E. Andronescu, *Dig. J. Nanomater. Bios.* **7**, 1639 (2012).
- [14] C. Gruian, H.-J. Steinhoff, S. Simon, *Dig. J. Nanomater. Bios.* **6**, 373 (2011).
- [15] T. Kokubo, H. Kushitani, S. Sakka, T. Kitsugi, T. Yamamuro, *J. Biomed. Mater. Res.* **24**, 721 (1990).
- [16] A.L. Patterson, *Phys. Rev.* **56**, 978 (1939).
- [17] A. Chrissanthopoulos, A. N Bouropoulos, S. N Yannopoulos, *Vib. Spectrosc* **48**, 118 (2008).
- [18] M. Mami, A. Lucas-Girot, H. Oudadesse, R. D Srid, F. Mezahi, E. Dietrich, *Appl. Surf. Sci.* **254**, 7386 (2008).
- [19] G.E. Stan, A.C. Popa, D. Bojin, *Dig. J. Nanomater. Bios.* **5**, 557 (2010).
- [20] G Socrates, *Infrared and Raman Characteristic Group Frequencies, Tables and Charts*, John Wiley and Sons, (Eds.), Ltd., Chichester, UK, (2001).
- [21] P. Innocenzi, *J. Non-Cryst. Solids* **316**, 309 (2003).
- [22] O.P. Filho, G.P. Latorre, L. L. Hench, *J. Biomed. Mater Res.* **30**, 509 (1996).
- [23] M.M. Pereira, A.E. Clark, L.L Hench, *J. Biomed. Mater. Res.* **28**, 693 (1994).
- [24] M.M. Pereira, A.E. Clark, L.L Hench, *J. Am. Ceram. Soc.* **78**, 2463 (1995).
- [25] C. Ohtsuki, M. Kamitakahara, T. Miyazaki, *J. Roy. Soc. Interface* **6**, S349 (2009).